Transmissive concentrator multijunction solar cells with over 47% in-band power conversion efficiency

Qi Xu¹, Yaping Ji¹, Dimitri D. Krut², Jim H. Ermer² and Matthew D. Escarra^{1,*}

¹Tulane University, New Orleans, LA, 70118, U.S.A.

²Boeing-Spectrolab Inc., Sylmar, CA, 91342, U.S.A.

*escarra@tulane.edu

Abstract: Transmissive concentrator multijunction (TCMJ) solar cells with over 47% in-band power conversion efficiency (PCE) have been designed and realized. These TCMJ solar cells have been characterized under 1 sun and concentrated 500 sun solar spectra, showing that the PCE for in-band light (photon energies above the cell's lowest bandgap) can reach up to 47.6% (29.5% for the full solar spectrum). Temperature coefficients of electrical parameters (V_{oc}, J_{sc}, FF) have been derived from measurements within the temperature range of 20° C to 130° C, showing linear variations versus temperature change. Optical measurements demonstrate that the cells show 76.5% solar-weighted optical transmission for the out-of-band light (photon energy below the cell's lowest bandgap). This TCMJ solar cell exhibits promising spectrum splitting capability, which has potential for use in hybrid photovoltaic-solar thermal applications.

Introduction

Solar cells composed of III-V materials have received significant attention in the last few decades for their excellent efficiency, high reliability, and widely tunable bandgaps. They are not only well known for their high performance in concentrator photovoltaic (CPV) modules¹⁻³, space-based applications^{4, 5}, and flexible formats⁶, but they also exhibit significant potential for being implemented in hybrid photovoltaic-solar thermal (PV/T) systems⁷⁻⁹. Many studies have shown that greater than 40% power conversion efficiency has been achieved in concentrator multijunction solar cells with bandgaps covering the ultraviolent (UV) to near-infrared (NIR) portions of the solar spectrum^{10, 11}, and these cells are typically used in CPV systems. However, these multijunction cells still do not absorb or utilize much of the NIR light, and in typical three-junction cells, thermalization of higher energy photons is still significant. To more fully utilize the full spectrum of incoming sunlight, it would be more suitable to split the solar spectrum in a hybrid PV/T system, where the higher energy (and therefore higher value) photons are directed to a multijunction solar cell that is tuned to those wavelengths, while the lost lower energy NIR photons are diverted to a solar thermal receiver, which absorbs these wavelengths with very high efficiency.

This paper describes the design and characterization of transmissive concentrator multijunction (TCMJ) solar cells that split the spectrum efficiently between PV conversion to electricity and thermal collection of NIR light. The thermal energy captured by such a system can be utilized on-demand as a dispatchable source of renewable electricity or process heat. As illustrated in Fig. 1(a), the cell absorbs the 'in-band light', the light whose energy is above the minimum bandgap of the TCMJ cells; meanwhile the 'out-of-band light', the light whose energy is below the minimum bandgap of the TCMJ cells, is transmitted straight through the cells to the thermal receiver. The in-band light absorbed in the cell (mainly the ultraviolet (UV) and visible light) is directly

converted to electricity with a power conversion efficiency around 47%, while the out-of-band light is transmitted with an optical efficiency over 76%. This spectrum splitting TCMJ solar cell has promising potential for a wide range of hybrid photovoltaic-solar thermal applications.

Cell Design

Figure 1(b) shows the schematic structure of the TCMJ solar cell. It consists of three sub-cells, with the following bandgaps (and material composition): 2.098eV (Al_{0.23}Ga_{0.26}In_{0.51}P) for C1, 1.675eV (Al_{0.18}Ga_{0.82}As) for C2, and 1.410eV (GaAs) for C3. The minimum bandgap selection of 1.410eV for C3 leads to an energy fraction of 0.62 for the in-band light and 0.38 for the out-of-band light. The materials and bandgaps for C1 and C2 are selected to provide photocurrent matching and lattice matching in the cell structure. GaAs is a convenient choice for C3 to provide fairly even splitting of the spectrum while allowing for growth on GaAs substrates. However, by utilizing epitaxial liftoff (ELO) to remove the substrate¹², a higher or lower cutoff bandgap may be chosen to vary the fraction of PV vs. solar thermal energy captured in the system.

Each sub-cell is composed of a window layer, emitter layer, base layer, and back surface field (BSF) layer. A low-doped, n-type GaAs (doping ~5e16 cm⁻³) substrate is employed to minimize parasitic absorption of transmitted out-of-band light and may be removed by epitaxial lift off (ELO) in the future. The TCMJ solar cells are epitaxially grown by metal-organic vapor phase epitaxy (MOVPE) and fabricated using standard III-V solar cell fabrication techniques¹¹, with the exception that the back contact is composed of a busbar and sparse grid fingers instead of a uniform metallic film. The cells are 5.5 mm×5.5 mm squares, with a thickness of 0.45 mm. The spacing of the electrode grid is 0.14 mm for the front and 0.28 mm for the rear; these are aligned to maximize overlap and minimize shadowing of transmitted out-of-band light. Grid fingers are 7 μm wide by 3.5 μm tall on the front and 9 μm wide by 5.5 μm tall on the back. A single busbar is utilized on each side that runs the length of the edge of the cell, with width of 180 μm. The fabrication also includes front-side and back-side anti-reflection coatings, where the front coating is designed to minimize reflection for the full spectrum (300 nm to 2500 nm), while the back coating is for the out-of-band light only (900 nm to 2500 nm); both coatings are designed to work for the wide range of incident angles of light that are incoming from the concentrator¹³.

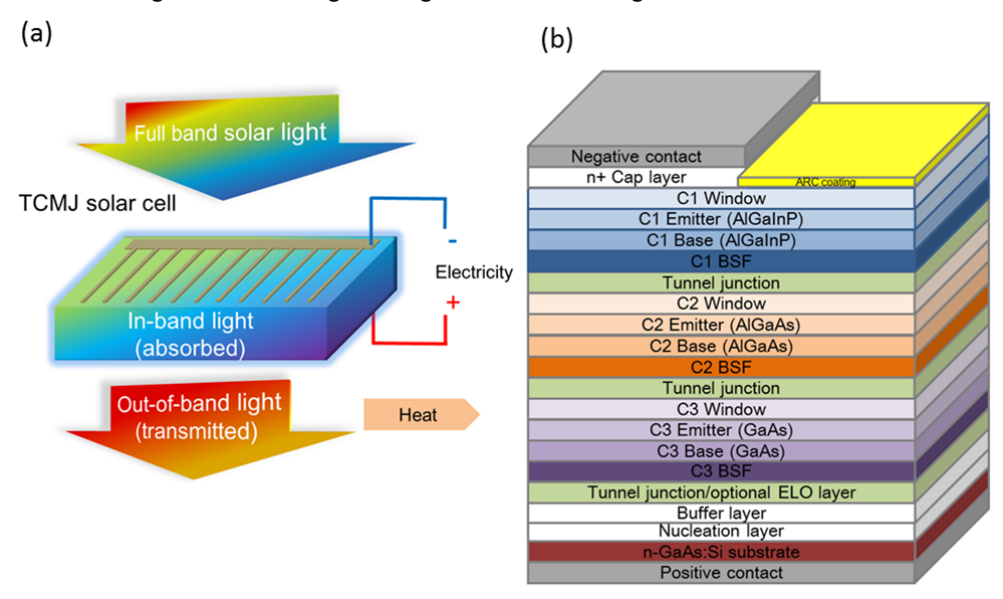


Fig. 1. (a) TCMJ solar cells more fully utilize the solar spectrum by splitting it – high energy photons are absorbed in the cell, while low energy photons are transmitted to a thermal receiver. (b) Schematic structure of the triple-junction solar cell (not to scale). The bandgap and composition of each sub-cell are C1: $2.098eV/Al_{0.23}Ga_{0.26}In_{0.51}P$; C2: $1.675eV/Al_{0.18}Ga_{0.82}As$; and C3: 1.410eV/GaAs.

Results and discussion

The illuminated I-V curves derived from the TCMJ solar cells under 1 sun and 500 suns are both shown in Fig. 2 for comparison. Both are measured at ~25°C. The 1 sun test is performed using a continuous, multi-zone solar simulator (Unisim, TS-Space Systems), with total intensity of 0.09W/cm². This simulator is calibrated to the AM1.5D spectrum by tuning two lamps and three LEDs (matched to the three bandgaps for these cells) to achieve the correct number of photons above each bandgap; this close AM1.5D match is confirmed using an independently calibrated UV/Vis/NIR fiber spectrometer (Ocean Optics). The concentrated 500 sun measurement is performed using a high-intensity, pulsed solar simulator (HIPSS, Spectrolab, Inc.), and the intensity is set to be 50W/cm², which is equal to 500 suns. Fig. 2 shows that the V_{oc} is 3.62V under 1 sun and increases up to 4.23V at 500 suns, while the Isc boosts dramatically from 2.39mA to 1.22A due to the highly concentrated incident light. The ratio of J_{sc} to the light intensity (J_{sc}/intensity) shows that the value is similar under both 1 sun (0.081A/W) and 500 suns (0.082A/W). Higher Voc at 500 suns scales logarithmically with the boost in photocurrent, as expected¹⁰. On the other hand, the fill factor (FF) of the cell drops from 87.0% to 82.6% under highly concentrated light, due to the increasing electrical resistance in the top and bottom grid contacts. The power conversion efficiency reaches 29.5% for the full spectrum of light under 500 suns, which corresponds to 47.6% efficiency for converting the in-band light with bandgap cutoff of 1.41eV. This latter efficiency metric is defined as

$$\eta_{inband} = rac{Electricity\ produced\ from\ cell}{Energy\ of\ incident\ light\ above\ 1.41eV}$$

and takes into account the separate use of the transmitted out-of-band photons for generating usable energy in a thermal receiver.

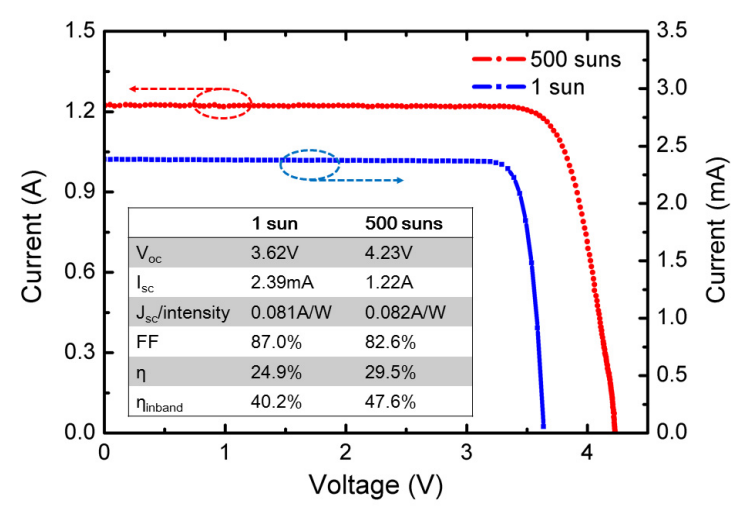


Fig. 2. Measured illuminated I-V characteristics for the TCMJ solar cells under 1 sun and the concentrated 500-sun AM1.5D spectrum, both at room temperature. Inset table: Electrical

parameters of the TCMJ solar cells. The area of the cells is 0.29 cm².

The high in-band efficiency enables the TCMJ solar cells to convert the UV and visible portions of the spectrum, which they are designed to capture, into electricity with very high efficiency. Compared to other conventional multijunction solar cells, such as germanium based ones, the in-band efficiency is very competitive^{10, 14}. The main difference between them is that the TCMJ solar cells shown here have a much higher bandgap cutoff, which enables the out-of-band light to transmit through the cell and be captured as heat rather than being converted to electricity. The cell temperature may be maintained below 110°C ¹⁵ while the thermal energy may be captured at temperatures up to 600°C. This will significantly increase the dispatchability of the solar energy in such a hybrid CPV/T system and provides higher exergy efficiency relative to low temperature CPV/T systems that capture heat directly from the cells ^{16, 17} Furthermore, the use of higher bandgap materials reduces thermalization losses in the cells and results in a higher voltage to bandgap ratio due to the fairly constant W_{oc} at these bandgaps¹⁸. This drives the high in-band efficiency of these devices.

The external quantum efficiency (EQE) of the TCMJ solar cells is measured at room temperature and exhibited in Fig. 3 (a). The bandgap for each subcell is verified to be 2.098eV (591nm) for C1, 1.675eV (740nm) for C2, and 1.410eV (879nm) for C3, respectively. An excellent current match between bandgaps is confirmed, with less than 0.7% mismatch.

These cells are anticipated to operate at temperatures up to 110°C in the field. In order to investigate the performance of the TCMJ solar cells at elevated temperatures, a temperature controlled stage (HFS600E, Linkam) is utilized with the 1-sun measurement to derive the temperature dependent I-V performance of the TCMJ solar cells. Measured results are plotted in Fig.3 (b), which shows a series of current density–voltage (J-V) curves from 20°C to 130°C . Due to the expected decrease in bandgap energy vs. temperature, the open-circuit voltage V_{oc} decreases with increasing temperature, while the short circuit current density J_{sc} increases as the temperature rises.

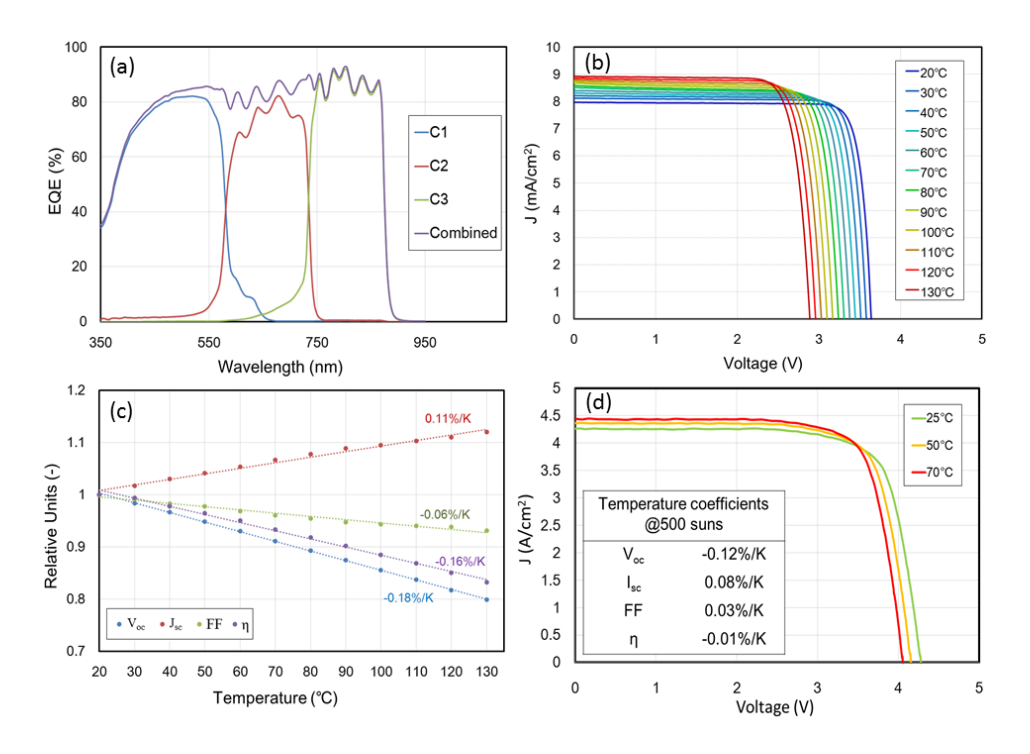


Fig. 3. (a) Measured external quantum efficiency (EQE) of the TCMJ solar cells. (b) Measured J-V curves for different temperatures under 1 sun. (c) Variance of cell performance parameters vs. temperature and associated temperature coefficients under 1 sun. (d) Measured J-V curves vs. temperature and relative temperature coefficients under 500 suns.

In order to gain further insight, the relative temperature coefficients of V_{oc} , J_{sc} , fill factor (FF) and the power conversion efficiency (η) under 1 sun are derived and exhibited in Fig. 3 (c). The V_{oc} decrease vs. increasing temperature shows linear variation, and the coefficient is measured to be -0.18%/K, which is similar to other values for III-V cells that are reported in literature^{1,19}. The J_{sc} slightly increases as the temperature goes up with a coefficient of 0.11%/K, showing a fairly linear response, with minimal evidence of additional current mismatch between junctions due to the shifting bandgap energies in this temperature range. On the other hand, the FF decreases at a rate of -0.06%/K when the temperature increases, leading to a similar decline in η at -0.16%/K. This results from an increase in the series resistance in the cell (sheet, contact, and electrode resistances).

Furthermore, J-V curves and relative temperature coefficients under 500 suns are also measured and shown in Fig. 3(d). The temperature coefficient of V_{oc} changes from -0.18%/K to -0.12%/K when the concentration rises from 1 sun to 500 suns, which is an expected decrease with concentration based on previous theoretical and experimental work¹⁹. I_{sc} increases vs. temperature at a similar rate (0.08%/K) as under 1 sun. On the other hand, the FF and η barely change vs. temperature when illuminated by 500 suns (with temperature coefficient of 0.03%/K and -0.01%/K, respectively), showing that the cell has fairly consistent efficiency across the operating temperature range and under expected concentration levels, as designed. The in-band cell efficiency at the expected operating temperature of 70°C and concentration of 500 suns is 47.1%. In addition to having high power conversion efficiency for in-band light, it is essential that the

TCMJ solar cell has high optical transmission efficiency for the out-of-band light as well. In order to investigate the optical performance, a white light source and a UV-Vis spectrometer (DH-2000, Ocean Optics) are employed. The measured and the calculated results are both shown in Fig. 4. The experiment matches our optical model, showing that the transmission is almost zero until 880nm (the bandgap cutoff, 1.41eV, for the triple junction cell), then dramatically increases to around 80% for the rest of the out-of-band solar spectrum. The oscillation in the experimental curve results from slight index mismatch and interference in the various epitaxial layers of the cell that is not accounted for in our optical model. By integrating the experimental transmission curve with the AM1.5D solar spectrum, the solar-weighted transmission efficiency is calculated to be 76.5% for the TCMJ solar cell. This value is promising for many applications; however, there are still a few factors that affect the transmission which may be improved, including further reduction in shadowing loss from the busbar and the grid electrodes on the cell and reduced free carrier absorption in the cell substrate and the tunnel junctions. In particular, it is believed that the transmission may be significantly enhanced by applying an ELO process to remove the GaAs substrate from the cell.

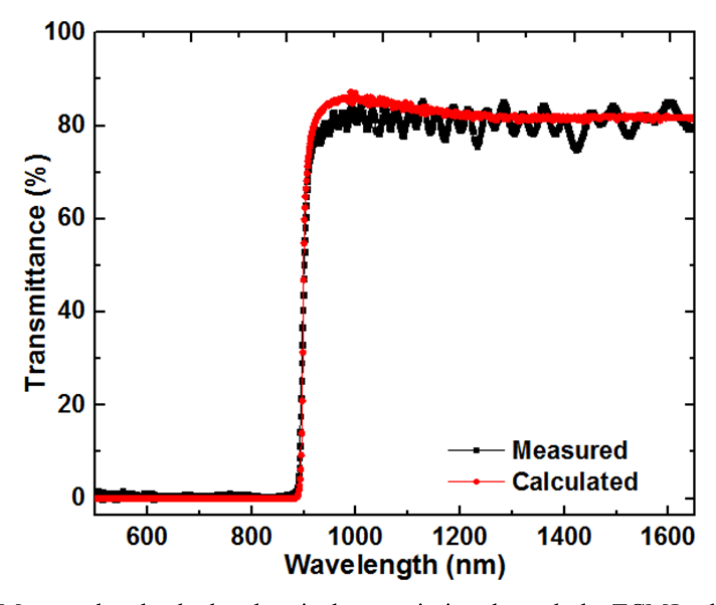


Fig. 4. Measured and calculated optical transmission through the TCMJ solar cells.

Conclusion

In summary, a transmissive concentrator multijunction (TCMJ) solar cell with 47.6% in-band power conversion efficiency (500 suns, 25°C) and 76.5% out-of-band optical transmission has been proposed and experimentally demonstrated. The cell has an in-band efficiency of 47.1% at the expected operating temperature of 70°C (under 500 suns). Temperature dependent measurements show that the electrical parameters (V_{oc} , J_{sc} , FF and η) vary linearly as the temperature increases and that the variations are in an acceptable range. The TCMJ solar cells exhibit promising potential for spectrum splitting applications, including deployment in a hybrid photovoltaic-solar thermal system with significant dispatchability (of heat or electricity) and high exergy efficiency.

Acknowledgement

The information, data, or work presented herein was funded in part by the Advanced Research Projects Agency-Energy, U.S. Department of Energy, under Award Number DE-AR0000473.

References

- 1. Gerhard Peharz, Juan P. Ferrer Rodríguez, Gerald Siefer and Andreas W. Bett, Prog Photovoltaics Res Appl 19, 54 (2011).
- 2. Eduardo F. Fernández, Pedro Pérez Higueras, Antonio J. Garcia Loureiro and Pedro G. Vidal, Prog Photovoltaics Res Appl 21, 693 (2013).
- 3. Xing Sheng, Christopher A. Bower, Salvatore Bonafede, John W. Wilson, Brent Fisher, Matthew Meitl, Homan Yuen, Shuodao Wang, Ling Shen and Anthony R. Banks, Nature materials 13, 593 (2014).
- 4. JA Carlin, SA Ringel, A. Fitzgerald and M. Bulsara, Solar Energy Mater. Solar Cells 66, 621 (2001).
- 5. Mark O'Neill, AJ McDanal, Henry Brandhorst, Kevin Schmid, Peter LaCorte, Michael Piszczor and Matt Myers, 1 (2015).
- 6. Katsuaki Tanabe, Katsuyuki Watanabe and Yasuhiko Arakawa, Appl. Phys. Lett. 100, 192102 (2012).
- 7. Ning Xu, Jie Ji, Wei Sun, Lisheng Han, Haifei Chen and Zhuling Jin, Energy Conversion and Management 100, 191 (2015).
- 8. J. Yu Zhengshan, Kathryn C. Fisher, Brian M. Wheelwright, Roger P. Angel and Zachary C. Holman, IEEE Journal of Photovoltaics 5, 1791 (2015).
- 9. David Cygan, Hamid Abbasi, Aleksandr Kozlov, Joseph Pondo, Roland Winston, Bennett Widyolar, Lun Jiang, Mahmoud Abdelhamid, AP Kirk and M. Drees, Materials Research Society MRS Advances (2016).
- 10. RR King, DC Law, KM Edmondson, CM Fetzer, GS Kinsey, H. Yoon, RA Sherif and NH Karam, Appl. Phys. Lett. 90, 183516 (2007).
- 11. JF Geisz, DJ Friedman, JS Ward, A. Duda, WJ Olavarria, TE Moriarty, JT Kiehl, MJ Romero, AG Norman and KM Jones, Appl. Phys. Lett. 93, 123505 (2008).
- 12. GJ Bauhuis, P. Mulder, EJ Haverkamp, JCCM Huijben and JJ Schermer, Solar Energy Mater. Solar Cells 93, 1488 (2009).
- 13. Yaping Ji, Adam Ollanik, Nicholas Farrar-Foley, Qi Xu, Leila Madrone, Pete Lynn, Vince Romanin, Daniel Codd and Matthew Escarra, 1 (2015).

- 14. Martin A. Green, Keith Emery, Yoshihiro Hishikawa, Wilhelm Warta and Ewan D. Dunlop, Prog Photovoltaics Res Appl 24, (2016).
- 15. Qi Xu, Yaping Ji, Brian Riggs, Adam Ollanik, Nicholas Farrar-Foley, Jim H.Ermer, Vince Romanin, Pete Lynn, Danny Codd and Matthew D. Escarra, Solar Energy 585 (2016).
- 16. Stephan Paredes, Brian Burg, Patrick Ruch, Ingmar Meijer and Bruno Michel, ERCIM NEWS 49 (2015).
- 17. Patrick Dupeyrat, Christophe Ménézo, Matthias Rommel and Hans-Martin Henning, Solar Energy 85, 1457 (2011).
- 18. RR King, D. Bhusari, A. Boca, D. Larrabee, X Q Liu, W. Hong, CM Fetzer, DC Law and NH Karam, Prog Photovoltaics Res Appl 19, 797 (2011).
- 19. Geoffrey S. Kinsey, Peter Hebert, Kent E. Barbour, Dmitri D. Krut, Hector L. Cotal and Raed A. Sherif, Prog Photovoltaics Res Appl 16, 503 (2008).

